

Collective effects in strong interaction processes: experimental highlights

V. A. Okorokov*

National Research Nuclear University MEPhI (Moscow Engineering Physics Institute), Kashirskoe highway 31, 115409 Moscow, Russia

(Dated: January 13, 2025)

Abstract—Collective effects are reviewed for collisions of various systems – from proton-proton to heavy ion – in wide energy range. In proton–proton interactions studies of hadron jets devote to the better understanding of some basic features of strong interaction and search for the physics beyond of Standard Model. First results have been obtained for massive gauge bosons and antitop-top pair production in proton–nuclear and heavy ion collisions at multi-TeV energies. The collectivity has been observed for various particle and beam species, in particular, in collision of small systems. Experimental results obtained for discrete symmetries of strong interaction at finite temperature confirm indirectly the topologically non-trivial structure of the vacuum. The recent measurements of femtoscopic correlations provide, in particular, the indirect estimations for parameters of hyperon-nucleon potentials which are essential for study of inner structure of compact astrophysical objects. Novel mechanism for multiparticle production due to collectivity can be expected in very high energy nuclear collisions and it may be helpful for better understanding of the nature of the muon puzzle in ultra-high energy cosmic ray measurements. Thus studies of collective effects in strong interaction processes provide new important results for relativistic astrophysics, cosmology and cosmic ray physics, i.e. have interdisciplinary significance.

PACS numbers: 12.38.Aw, 12.38.Qt, 25.75.–q, 26.60.–c

I. INTRODUCTION

There is no full and self-consistent theory of strong interaction despite of significant progress during last decades. The general and well-established picture of strong interaction reaction [1] leads to the hypothesis that collective behavior and corresponding effects are deeply intrinsic properties of strong interaction driven by the dynamics of the collision process at all stages of its space-time evolution. As consequence, investigations of collective effects and collective modes of excitation of the hadronic / quark-gluon matter provide unique information and are among the most promising and relevant for constructing a complete theory of strong interaction and studying of quantum multiparticle systems. The study of collective and correlation characteristics of strong interaction makes it possible to draw conclusions regarding the space-time evolution of the interaction process and to establish a fundamental relationship between the geometry and dynamics of the creation of a final state.

During XXI century the main part of experimental and theoretical studies within strong interaction physics is based on the research works making at Relativistic Heavy Ion Collider (RHIC) and the Large Hadron Collider (LHC). Therefore the consideration below is focused on the results obtained at these facilities. The accelerator complex RHIC was designed and was built for investigations in Quantum chromodynamics (QCD) field specially. There were 24 successful physics runs since 2000 year. Runs 25 and 26 are planed. The following large detectors are placed at RHIC: STAR continue to collect new data since 2000, sPHENIX was commissioned in 2023. Data were also taken by small experiments BRAHMS, PHOBOS and by large one PHENIX. Table I shows the data samples collected during 24 runs at RHIC, where $\sqrt{s_{NN}}$ is the center-of-mass energy per nucleon–nucleon pair. The sPHENIX and STAR detectors are characterized by good particle identification and uniform, large acceptance. Thus both RHIC detectors are suitable rather good for study of various collective effects. The accelerator complex LHC was designed and was built for investigations in fundamental physics, in particular, in subfield of QCD. There were 2 successful physics runs since 2009 year, the run 3 is in the progress¹. The large detectors ALICE, ATLAS, CMS and LHCb are placed at the LHC and they collect data since 2009. There also are wide set of smaller experiments focused on the specific issues in fundamental physics. The data samples taken at the LHC since 2009 are shown in Table II. ALICE, ATLAS and CMS are a general-purpose detectors characterized by good particle identification and (quasi)uniform, large acceptance. Designs of all of these detectors are well optimized for study of wide sets of collective effects. Nevertheless the LHCb is

*Electronic address: VAOkorokov@mephi.ru; Okorokov@bnl.gov

¹ It should be emphasized the run at the LHC implies the multi-year period of work of the accelerator, namely, run 1 was during 2009–2013 years, run 2 – 2015–2018 years, run 3 is planned on 2022–2025 years.

TABLE I: Data samples obtained during RHIC runs.

Species	$\sqrt{s_{NN}}$, GeV
$p + p^a$	22.0 ^b , 62.4, 200, 410 ^b , 500, 510
$p + \text{Al}$	200
$\text{O} + \text{O}$	200 ^b
$p^a + \text{Au}$	200
$\text{d} + \text{Au}$	19.6, 39.0, 62.4, 200
$\text{He}^3 + \text{Au}$	200
$\text{Al} + \text{Au}$	4.9 ^{b,c} , 200
$\text{Cu} + \text{Cu}$	22.4 ^b , 62.4, 200
$\text{Cu} + \text{Au}$	200
$\text{Zr} + \text{Zr}, \text{Ru} + \text{Ru}^d$	200
$\text{Au} + \text{Au}$	FXT ^c : 3.0, 3.2, 3.5, 3.9, 4.5, 5.2, 6.2, 7.2, 7.7 7.7, 9.2 ^b , 11.5, 14.6, 17.3, 19.6, 27.0, 39.0, 54.4 ^b , 55.8 ^b , 62.4, 130, 200
$\text{U} + \text{U}$	193

^a with unpolarized ($\sqrt{s} = 62.4$ GeV) and with longitudinal / transverse polarized beams; ^b run with small integral luminosity; ^c run for STAR fixed target mode; ^d run with isobar beams

TABLE II: Data samples obtained during LHC runs.

Species	$\sqrt{s_{NN}}$, GeV
$p + p$	900, 2360, 2760, 5020, 7000, 8000, 13000, 13600
$p + \text{Pb}$	5020, 8160
$\text{Xe} + \text{Xe}$	5440
$\text{Pb} + \text{Pb}$	2760, 5020, 5360

single-arm spectrometer an important results have been already obtained for femtoscopic correlations and jet physics with this apparatus.

II. SOME RESULTS FOR COLLECTIVITY

The section contains separate important results obtained within very extensive studies of various collective effects which are described in details in some recent reviews [2–6].

A. Hadronic jets

The development of experimental technique and data analysis results in the possibility for full reconstruction of jets created not only in hadronic, mostly (anti)proton–proton ($p + p$, $\bar{p} + p$) beam interactions, but also in nucleus–nucleus ($A + B$) collisions.

In $p + p$ the measurements for inclusive jet and dijet cross sections are extended to the multi-TeV region for kinematic parameters, namely, up to jet transverse momentum $p_T^J \approx 4$ TeV/ c and dijet mass $m_{JJ} \approx 10$ TeV/ c^2 [4]. Overall, fair agreement between the measured cross sections (that span several orders of magnitude) and the fixed-order pQCD calculations in next-to-next-to-leading order (N²LO), corrected for non-perturbative and electroweak effects, is observed. The evolution of the strong coupling as a function of the energy scale, $\alpha_S(Q)$ has been tested with help of the ratio observable $R_{\Delta\phi}(p_T^J)$, related to the azimuthal correlations among jets up to $Q \approx 2$ TeV/ c , a higher scale than that probed in previous measurements [6]. The $\alpha_S(m_Z)$ has been recently determined with help of the energy correlators inside jets using an event sample of $\sqrt{s} = 13$ TeV $p + p$ collisions. The measured distributions are consistent with the trends in the simulation that reveal two key features of the strong interaction: confinement and asymptotic freedom, the strong coupling is $\alpha_S(m_Z) = 0.1229^{+0.0040}_{-0.0050}$ [7]. This result is the most precise $\alpha_S(m_Z)$ value obtained using jet substructure observables and it is consistent with the world average $[\alpha_S(m_Z)]_{\text{wa}} = 0.1180 \pm 0.0009$ [8]. The pattern of the parton shower is expected to depend on the mass of the initiating parton, through a phenomenon known as the dead-cone effect, which predicts a suppression of the gluon spectrum emitted by a heavy quark of mass m_Q and

energy E_Q , within a cone of angular size m_Q/E_Q around the emitter. The QCD dead cone was directly measured in $p + p$ collisions at $\sqrt{s} = 13$ TeV with the significances of 7.7σ , 3.5σ and 1.0σ for $5 < E_Q < 10$ GeV, $10 < E_Q < 20$ GeV and $20 < E_Q < 35$ GeV, using iterative declustering of jets tagged with a fully reconstructed D^0 -meson [3]. These results provide direct sensitivity to the mass of quasi-free c quarks, before they bind into hadrons and pave the way for a study of the mass dependence of the dead-cone effect, by measuring the dead cone of b -tagged jets with a reconstructed beauty hadrons. The energy frontier provides many unique approaches and discovery opportunities for physics beyond Standard Model (SM) – BSM physics. A study of jets in $p + p$ collisions is focused, in particular, on the search for the BSM physics within Effective Field Theory (EFT) approach for top quark (t) sector up to ultra-high energies [9, 10]. The sensitivity to dijet resonances in $p + p$ is intensively explored regarding of the projects future collider with proton beams at different energies up to $\sqrt{s} = 500$ TeV [11, 12]. The discovery mass reach of a proton–proton collider is $m_{JJ} \approx \kappa\sqrt{s}$ with $\kappa = 0.5$ for strongly produced dijet resonances, $\kappa = 0.25$ for weakly produced ones [12].

In [13] it was pointed out that behavior of Higgs boson (h) in the quark-gluon matter at finite temperature (T) called also (strongly coupled) quark-gluon plasma – (s)QGP² – could be studied at future multi-TeV colliders. At present h and t are widely considered as important probes of a pre-equilibrium stages of space-time evolution of QGP in domain of high and ultra-high collision energies [9, 10]. Datasets with large integrated luminosities obtained at the LHC for $p + \text{Pb}$ at $\sqrt{s_{NN}} = 8.16$ TeV and $\text{Pb} + \text{Pb}$ at $\sqrt{s_{NN}} = 5.02$ TeV result in the reconstruction of $t\bar{t}$ events in the (a) dilepton (l^+l^-), (b) $l^+l^- + 2$ jets and (c) $l^\pm + 4$ jets channels become accessible experimentally, where $l^\pm = e^\pm, \mu^\pm$. For $p + \text{Pb}$ at $\sqrt{s_{NN}} = 8.16$ TeV the most precision result is obtained by ATLAS. Combining both (b) and (c) channels, the $t\bar{t}$ pair production cross section is measured to be $\sigma_{t\bar{t}}^{p+\text{Pb}} = (58.1 \pm 2.0^{+4.8}_{-4.4})$ nb, where the first uncertainty is statistical and second one is systematic [14]. Cross sections measured by ATLAS and CMS [15] are found to be in good agreement each other and with SM predictions. Precision of these measurements opens a new way to constraint parton distribution functions (PDFs) in the high- x region. For $\text{Pb} + \text{Pb}$ at $\sqrt{s_{NN}} = 5.02$ TeV the first measurements by CMS are $\sigma_{t\bar{t}}^{\text{Pb}+\text{Pb}} = (2.5^{+0.8}_{-0.7}) \mu\text{b}$ and $(2.0^{+0.7}_{-0.6}) \mu\text{b}$ utilizing the leptons only and in the channel (b) with the b quarks respectively [16], ATLAS obtained the result $\sigma_{t\bar{t}}^{\text{Pb}+\text{Pb}} = (3.6^{+1.0+0.8}_{-0.9-0.5}) \mu\text{b}$ using the channel with $e\mu$ and at least two jets [17]. The corresponding values of $\sigma_{t\bar{t}}^{\text{Pb}+\text{Pb}}$ obtained by ATLAS and CMS agree within uncertainties for channel (b). For the first case experimental result is consistent with theoretical predictions using a range of different nuclear PDFs. On the other side, the values extracted by CMS are compatible with, though somewhat lower than, the expectations from scaled $p + p$ data and pQCD calculations. The observation of $t\bar{t}$ production consolidates the evidence of the existence of all quark flavors in the pre-equilibrium stage of the QGP at very high energy densities, similar to the conditions present in the early Universe [17].

Jet quenching is considered as one of the most promising signatures of formation of the QGP and sensitive probe for transport properties of final-state matter. Experiments at the LHC extend the measurements for jet quenching up to $p_T \approx 1$ TeV/ c . The nuclear modification factor (R_{AA}) exhibits larger suppression for jets than hadrons at the same p_T , with the ALICE jet spectrum extending down to $p_T = 60$ GeV/ c . At higher p_T the ALICE and ATLAS jet data are consistent, and show slowly increasing R_{AA} with increasing p_T [3]. In $\text{Pb} + \text{Pb}$ collisions at $\sqrt{s_{NN}} = 5.02$ TeV the γ - and b -tagged jets are less suppressed than the inclusive jets at $p_T^J < 0.2$ TeV/ c , implying that the energy loss depends on the color charge and possibly the mass of the parton. Suppression measurements in the heavy-flavour sector at intermediate p_T for nuclear collisions indicate that b quarks lose less energy than c quarks. These measurements are described by models that include mass-dependent elastic energy loss and a reduction of gluon radiation off heavier quarks, i.e. the QCD dead-cone. Several collaborations also study the shift in p_T needed to match the $A + A$ spectra to that of the binary scaled $p + p$. Such analysis show that at LHC energies $(\Delta p_T)_q \text{ dominated} < (\Delta p_T)_g \text{ dominated}$ and $(\Delta p_T)_{\text{RHIC}} < (\Delta p_T)_{\text{LHC}}$. In particular, jet energy loss has been measured by ALICE experiment for the semi-inclusive distribution of jets recoiling from a hadron trigger to be $\Delta p_T = (8 \pm 2)$ GeV/ c for central $\text{Pb} + \text{Pb}$ collisions. This value is larger than that determined from similar analysis at RHIC, though the comparison currently has limited significance [3].

² It should be noted that accelerator complexes, at least, commissioned at present allow the study of strongly coupled QGP. Therefore, within the paper the abbreviation QGP is used if it is discussed the corresponding state of strongly interacting matter in general. The abbreviation sQGP is used if it is considered the state of quark-gluon matter available for experimental study at present.

B. Collective flows and chiral effects

The geometrical shape of the impact region of two colliding subatomic particles can be quantified by the Fourier decomposition of the invariant distribution of the final-state particles, which, in general case, is [18, 19]

$$E \frac{d^3 N_\alpha}{d\mathbf{p}} = \frac{1}{2\pi} \frac{d^2 N_\alpha}{p_T dp_T dy} \left[1 + 2 \sum_{n=1}^{\infty} \{v_{n,\alpha} \cos(n\Delta\phi_\alpha) + a_{n,\alpha} \sin(n\Delta\phi_\alpha)\} \right]. \quad (1)$$

Here $\Delta\phi_\alpha \equiv \phi_\alpha - \Psi_{\text{RP}}$, ϕ_α is an azimuthal angle of particle with certain sign of electric charge α ($\alpha = +, -$) under study, Ψ_{RP} – azimuthal angle of reaction plane, $v_{n,\alpha}$ – collective flow of n -th order, the parameters $a_{n,\alpha}$ describe the effect of possible \mathcal{P}/\mathcal{CP} violation.

Identified light hadron flow measurements have been performed for a variety of collision systems recently. At RHIC, these include collisions of Y + Au at $\sqrt{s_{NN}} = 200$ GeV with Y $\equiv p, d, {}^3\text{He}^{2+}$, Cu and U + U at $\sqrt{s_{NN}} = 193$ GeV, while at the LHC these include Xe + Xe at $\sqrt{s_{NN}} = 5.44$ TeV. They have also been explored for higher orders of anisotropic flow, with examples from RHIC for Au + Au collisions at $\sqrt{s_{NN}} = 200$ GeV, and Pb + Pb collisions at $\sqrt{s_{NN}} = 5.02$ TeV. A hallmark of the hydrodynamic response is the mass ordering observed for the p_T -dependence of elliptic flow (v_2) of various hadron species in the light flavor sector [2]. Through detailed studies of azimuthal anisotropy coefficients $v_{n \geq 2}$ the CMS data impose stringent constraints on the allowed range of the shear viscosity-to-entropy ratio $\tilde{\eta}/s = 0.08 - 0.20$. This reaffirms that the sQGP behaves like a “nearly perfect liquid”, exhibiting minimal frictional momentum dissipation. Hydrodynamic calculations can also describe measurements of higher-order flow coefficients (up to v_8), non-linear contributions to higher-order flow coefficients, and symmetry plane correlations. On the other hand, for reasons subject to much theoretical attention, hydrodynamic predictions cannot describe measured anisotropic flow coefficients at LHC energies in ultra central Pb + Pb collisions to the same degree of accuracy as mid-central Pb + Pb interactions. The J/ψ v_2 measured in Pb + Pb collisions at $\sqrt{s_{NN}} = 5.02$ TeV by ALICE increases with p_T and reaches about 0.1 around $p_T = 5$ GeV/ c . Such a large v_2 signal at low to intermediate p_T can only be explained by the dominance of regenerated J/ψ mesons inheriting the elliptic flow of the constituent charm quarks which likely have reached local thermalization in the QGP [2]. This observation constitutes a proof of deconfinement, as it implies that coloured partons can move freely over distances much larger than the hadronic scale [3].

The c quarks are formed at the earliest stages of the collision, and therefore will have to overcome much larger magnetic fields than charged particles. The asymmetry measured by STAR for v_1 shows no charge asymmetry within the uncertainties and ALICE observes linear dependence with pseudorapidity (η) for the differences of the charge-dependent v_1 , denoted as Δv_1 , in mid-central Pb + Pb collisions at $\sqrt{s_{NN}} = 5.02$ TeV for charged particles and D^0, \bar{D}^0 mesons. The slope $d\Delta v_1/d\eta$, extracted with a linear fit function, yields $(1.68 \pm 0.49 \pm 0.41) \times 10^{-4}$ for charged hadrons with $p_T > 0.2$ GeV/ c for the 5–40% centrality interval and $(4.9 \pm 1.7 \pm 0.6) \times 10^{-1}$ for D^0 mesons with $3 < p_T < 6$ GeV/ c in a centrality interval of 10–40%, resulting in a significance of 2.6σ and 2.7σ for having a positive value, respectively. This measurement constitutes the first experimental hint of the existence of the initial state electromagnetic fields at the LHC [3]. The differences in the measured global polarisation of Λ and $\bar{\Lambda}$ provide an upper limit for the magnitude of the magnetic field at freeze-out of 5.7×10^{12} T and 14.4×10^{12} T at a 95% confidence level (CL) in Pb + Pb collisions at $\sqrt{s_{NN}} = 2.76$ and 5.02 TeV, respectively [3].

Atomic nuclei manifest a variety of shapes. In [20] the collective-flow-assisted nuclear shape-imaging method was introduced and used for the study of the shape of ground-state ${}^{238}\text{U}^{92+}$ nuclei. It was found a large deformation with a slight deviation from axial symmetry in the nuclear ground state, aligning broadly with previous low energy experiments [20].

The strong evidence was found for collectivity through multiparticle correlation analyses in $p + p$ and $p + \text{Pb}$ collisions at the LHC energies. Studies of particle correlation functions have been extended by CMS to the even smaller $\gamma + \text{Pb}$ collision system, using $p + \text{Pb}$ UPCs. The $\gamma + \text{Pb}$ data are consistent with predictions of models that do not include any collective effects. Measurements of prompt D^0 and J/ψ mesons in $p + p$ and $p + \text{Pb}$ collisions at the LHC energies suggest a weaker collectivity signal for c quarks than for light quarks. The study of c quark collectivity indicates positive v_2 , even in low-multiplicity $p + \text{Pb}$ collisions, while heavier bottom hadrons are found to have weaker collective signals, at a level that is currently not detected conclusively, than those of light flavor hadrons [5]. The presence of a jet was shown to alter the $v_n(p_T)$ in the range of $p_T \sim 2 - 10$ GeV in $p + \text{Pb}$ collisions. Thus, collective flow observables in this p_T range in small systems provide an intriguing possibility to better understand jet-medium interactions [2].

In a system that is not invariant under a parity transformation (i.e., chiral), a electromagnetic current and electric dipole moment of QCD matter can be induced by an external magnetic field, such as generated in the passage of two (heavy) nuclei. The resulting charge separation can be identified by studying the \mathcal{P}/\mathcal{CP} -odd sine terms in (1). The experimental manifestation of the local topologically induced \mathcal{P}/\mathcal{CP} violation in strong interaction is phenomenon

called chiral magnetic effect (CME). The correlator used for study of CME can be generalised according to [3]: $\gamma_{m,n} = \langle \cos[m\phi_\alpha + n\phi_\beta - (m+n)\Psi_{|m+n|}] \rangle$, $\delta_m = \langle \cos[m(\phi_\alpha - \phi_\beta)] \rangle$, $m, n \in Z$ and $\Psi_{|m+n|}$ is the azimuthal angle of the symmetry plane of $|m+n|$ -th order. The presence of a net positive electric charge can induce a positive axial current along the direction of the magnetic field i.e., leading to flow of chirality. This is caused by the chiral separation effect (CSE) [19]. The coupling between the CME and the CSE leads to a wave propagation of the electric charge, resulting in an electric charge quadrupole moment of the system, the chiral magnetic wave (CMW) [19]. The azimuthal distribution of charged particles due to the presence of the CMW can be written as $dN^\pm/d\phi = N^\pm \{1 + (2v_2 \mp rA) \cos[2(\phi - \Psi_2)]\}$, where $A = (N^+ - N^-)/(N^+ + N^-)$ is the charge asymmetry, and r is the parameter that encodes the strength of the electric quadrupole due to the CMW [3]. Therefore, one can probe the value of r by measuring the v_2 values for different charges as a function of the charge asymmetry. Instead, it was suggested to measure the covariance of v_n and A that is a robust observable and does not depend on detector inefficiencies.

Isobaric collisions were proposed to study two systems with similar v_2 but different magnetic field strengths, such as $^{96}\text{Ru}^{44+}$ and $^{96}\text{Zr}^{40+}$. The STAR extracted an upper limit of the CME fraction of approximately 10% at a 95% CL in isobar collisions at $\sqrt{s_{NN}} = 200$ GeV [21, 22]. On the other hand, the Au + Au collision data from STAR indicate a possible finite CME signal [23]. This is consistent with the expectation that the signal-to-background ratio is approximately a factor of three larger in Au + Au collisions than in isobar collisions. Measurements of $\Delta\gamma_{1,1} = \gamma_{1,1}^{\text{OS}} - \gamma_{1,1}^{\text{SS}}$ at RHIC and LHC energies are qualitatively consistent with the CME expectation, where $\gamma_{1,1}^{\text{OS/SS}}$ denotes the $\gamma_{1,1}$ with opposite (OS) / same (SS) sign particle pair and the quantity $\Delta\gamma_{1,1}$ assumes reduce of mutual backgrounds [18, 19]. One of the difficulties in interpreting the positive $\Delta\gamma_{1,1}$ is whether the CME is the major charge-dependent background contribution to the observable, such as those from resonance decays and jets [24]. Using the event shape engineering (ESE) method, the ALICE experiment showed that the CME fraction in the measured $\Delta\gamma_{1,1}$ is consistent with zero in Pb+Pb collisions at $\sqrt{s_{NN}} = 2.76$ TeV. The contribution from the CME to the measurement of charge dependent correlations relative to the second order symmetry plane ($\gamma_{1,1}$) is constrained to an upper limit of 15–33% in Pb + Pb and 2% in Xe + Xe collisions at the LHC energies at 95% CL [3]. The combination of the second and third harmonic results for CMW studies at the LHC indicates a significant background contribution from local charge conservation [3]. The CMS results obtained for small systems unambiguously demonstrate that the CME and CMW signals in nuclear collisions are too small to be observed at the LHC energies. The most stringent upper limit to date has been set on the CME signal which is estimated to be 13% in $p + \text{Pb}$ at $\sqrt{s_{NN}} = 8.16$ TeV and 7% in Pb + Pb collisions at $\sqrt{s_{NN}} = 5.02$ TeV, at 95% CL [5].

C. Femtoscopic correlations and Bose–Einstein condensation

The correlations at low relative momentum, called also as femtoscopic correlations, emerge due to both the symmetrization requirement of quantum statistics (QS) and the effect of final state interaction (FSI) among particles of the system under consideration. Experimentally, correlation function (CF) in general case of n -particle system is defined as the ratio $C_n = \zeta \mathcal{N}_s / \mathcal{N}_m$, where the quantities are the functions of the set $\{p_i\}_{i=1}^n \equiv (p_1, \dots, p_n)$ of 4-momenta p_i , $i = 1, \dots, n$ for secondary particles, \mathcal{N}_s and \mathcal{N}_m represent the distributions for particles produced in the same and in different collisions, respectively, ζ denotes the corrections for all experimental effects (acceptance, particle identification etc.). At present the correlations of identical particles with low relative momenta are mostly used for study of space-time extents of fireball. The main part of experimental data are obtained for pairs of π^\pm , also there are some results for pp ($\bar{p}\bar{p}$), neutral particle (γ , π^0 , K^0 , Λ) and charged kaon pairs. The FSI effect allows for the correlation femtoscopy with unlike particles the access, in particular, to a study of strong interactions between specific particles. This issue is in the focus below.

The strong potentials predicted for the four allowed spin and isospin states of the $p - \Xi^-$ system can be found elsewhere [25]. It was obtained that for all cases, an attractive interaction and a repulsive core characterize the potentials. The total $p - \Xi^-$ CF measured in $p + p$ collisions at $\sqrt{s} = 13$ TeV recorded with a high-multiplicity trigger by ALICE lies above the Coulomb predictions as well as the CF for $p - \Omega + \bar{p} - \bar{\Omega}$ [3], demonstrating the presence of an additional attractive strong interaction between p and multistrange hyperons. The $p - \Omega + \bar{p} - \bar{\Omega}$ CF measured by STAR in Au + Au collisions at $\sqrt{s_{NN}} = 200$ GeV does not allow to extract the interaction parameters due to limited statistics. However, based on the comparison of experimental results and model predictions for CF, one can conclude that data obtained by STAR favor a positive scattering length for the $p - \Omega$ interaction [26]. The positive scattering length and the measured ratio of the $p - \Omega + \bar{p} - \bar{\Omega}$ CFs from peripheral to central collisions less than unity for $k^* < 40$ MeV/ c within 1σ favors the $p - \Omega$ interaction potential with deep $p - \Omega$ bound state and binding energy $E_b \sim 27$ MeV for p and Ω , where $k^* = |\mathbf{p}_1^* - \mathbf{p}_2^*|/2$ is the absolute value of relative 3-momentum of one of the particles in the pair rest frame. Baryon-antibaryon correlations were studied in $p + \bar{p}$ and Pb + Pb collisions at the LHC and the real and imaginary part of the scattering parameters for $p - \Lambda$ and $\Lambda - \bar{\Lambda}$ were extracted for the first time [3].

Knowledge regarding the interaction of hyperons with nucleons is one of the key ingredients needed to understand the

composition of the compact astrophysical objects, in particular, neutron stars (NSs). The high-density environment ($\rho \approx 3 - 4\rho_0$) that is supposed to occur in the interior of NSs leads to an increase in the Fermi energy of the nucleons, translating into the appearance of new degrees of freedom, such as hyperons. The inclusion of hyperons leads to NS configurations that cannot reach the current highest mass limit from experimental observations of $2.2M_\odot$. For this reason, the presence of hyperons inside the inner cores of NSs is still under debate, and this so-called hyperon puzzle is far from being solved [25]. A major advance in understanding the role played by heavier strange hadrons in the hyperon puzzle has been achieved by the validation of lattice QCD predictions for the $N\Xi$ interaction by the aforementioned experimental results for $p - \Xi$ correlations. Mass-radius relationship $M(R)$ for the EoS scenario taking into account the constraints from the recent accelerator data for $p - \Xi$ interaction agree reasonably with the astrophysical measurements of heavy NSs [25]. In particular, this EoS allows the existence of heavy NS with $M > 2M_\odot$ at radii within the narrow range 11.5–12.5 km, which is fully compatible with the recent measurements of NSs close to and above two solar masses [25].

System with arbitrary number of bosons can undergo a Bose–Einstein condensation (BEC) due to statistical properties of quantum system and symmetry of the wave function (WF) of a boson state. Regarding the multiparticle production process the increasing the number density of bosons or increasing the overlap of the multi-boson wave-packet states, achieved by changing the size of the single-particle wave-packets lead to condensation of bosons into the same quantum state and bosonic (pion) laser could be created. The first case is the pion laser model (PLM) [27] and second approach is called generalized pion laser model (gPLM) [28, 29].

The coherent emission can be considered as one of the experimental signals of the appearance of BEC. Search for coherent pion emission was studied with help of multiparticle correlations within femtoscopy in $p+p$, $p+Pb$ and $Pb+Pb$ at the LHC energies [30]. The measured same-charge multipion correlations are compared to the expectation from lower-order experimental CFs. There is no a significant suppression of 4-pion correlations in $p+p$ or $p+Pb$ collisions, although the unknown strength of the nonfemtoscopic background prevents an absolute statement. A significant suppression of multipion Bose–Einstein correlations has been observed in $Pb+Pb$ collisions at $\sqrt{s_{NN}} = 2.76$ TeV. A coherent fraction of about $0.32 \pm 0.03 \pm 0.09$ could largely explain the 4 pion suppression, but the same value cannot explain the 3 pion suppression. Thus the origin of the suppression is not clear and the effect may be explained by postulating either coherent pion emission or large multibody Coulomb effects [30].

Within phenomenological studies of BEC in strong interaction processes [31–33] the particle density is defined as follows: $n_{ch} = N_{ch}/V$, where N_{ch} is the total charged particle multiplicity, V – estimation for the volume of the emission region of the boson under consideration (pions). The physical quantities in r.h.s. of the above equation – N_{ch} and V – are model-dependent. The critical value for n_{ch} can be calculated with help of the equation above and transition to the critical total multiplicity. The following relation

$$N_{ch,c} = \frac{1}{N_{\pi,(1)}} \left[\frac{1 + X + \sqrt{1 + 2X}}{2} \right]^{3/2}, \quad (2)$$

$$X \equiv 2m_\pi T_{\text{eff}} R_{\text{eff}}^2, \quad T_{\text{eff}} = T + \frac{\Delta_p^2}{2m_\pi}, \quad R_{\text{eff}}^2 = R_m^2 + \frac{T}{2\Delta_p^2 T_{\text{eff}}}.$$

is suggested elsewhere [33] for the critical value of N_{ch} for 3D case based on the gPLM. Here T_{eff} and R_{eff} is effective temperature and radius of the source, Δ_p is the momentum spread of the emitted pions, $N_{\pi,(1)} = 0.25$ is the fraction of the 1-st generation pions to be emitted from a static Gaussian source within unit of η , R_m is the estimation of the source radius, $T \approx T_{ch}$ is the source temperature supposed equal to the value of the parameter at chemical freeze-out [31–33]. The energy-dependent average N_{ch} in $p+p$ collisions is approximated by functions $\langle N_{ch}^{pp} \rangle_1 \propto \varepsilon^{0.29}$ and $\langle N_{ch}^{pp} \rangle_2 = \langle N_{ch,F} \rangle + N_0$ described in details elsewhere [33], where $\langle N_{ch}^{pp} \rangle_2$ was inspired by pQCD and $\varepsilon \equiv s/s_0$, $s_0 = 1$ GeV². For $A+A$ collisions the functions $\langle N_{ch}^{AA} \rangle_1 \propto \varepsilon_{NN}^{0.55}$ and $\langle N_{ch}^{AA} \rangle_2 \propto \varepsilon_{NN}^{0.15} \ln \varepsilon_{NN}$ are recently used [33]. In the case of the Poissonian distribution with mean n_0 for the multiplicity of secondary bosons the influence of the BEC results in the modified probability distribution for the special case of the rare Bose gas [29], i.e. $X \gg 1$, with the mean value $n(X) = n_0[1 + n_0(2X)^{-3/2}]$. Phenomenological studies of possible manifestation of BEC in various strong interaction processes [31–33] prove that $\langle n_{ch} \rangle$ in $p+p$ is smaller than its critical value up to $\sqrt{s} \sim 1$ PeV for any used views of $\langle N_{ch}^{pp} \rangle$. In heavy ion $A+A$ collisions n_{ch} larger than its critical value at any energies $10^{17} \leq E_N \leq 10^{21}$ eV in laboratory reference system (l.r.s.) for any approximations of $\langle N_{ch}^{AA} \rangle$ considered in [32, 33]. The BEC results in to the visible increase of charged particle density at even large enough $X = 5$ for the energy range with $\langle n_{ch}^{AA} \rangle > \langle n_{ch,c}^{AA} \rangle$. The absence of clear manifestation of BEC in $Pb+Pb$ collisions at $\sqrt{s_{NN}} = 2.76$ TeV well agrees with the conclusion within gPLM [33]. The characteristics

$$z_\pi^{(n)} = \frac{\ln \langle n_{ch,BEC}^{AA} \rangle - \ln \langle n_{ch,0}^{pp} \rangle}{\ln \langle n_{ch,0}^{AA} \rangle - \ln \langle n_{ch,0}^{pp} \rangle}, \quad \Delta z_\pi^{(n)} = z_\pi^{(n)} - 1. \quad (3)$$

determined in [33] are used for quantitative study of the effect of BEC on the density of secondary charged pions. Here $\langle n_{\text{ch,BEC}}^{AA/pp} \rangle$ is the average density of charged pions with taking into account the possible BEC at the region of (kinematic) parameter space with $\langle n_{\text{ch}} \rangle > n_{\text{ch,c}}$ in $A + A$ or $p + p$ collisions respectively, $\langle n_{\text{ch,0}}^{AA/pp} \rangle$ is the average particle density when the BEC is switched off in the fixed type interaction³.

Fig. 1 shows energy dependence of $z_{\pi}^{(n)}$ (a, b) and $\Delta z_{\pi}^{(n)}$ (c, d) for all possible combinations of approximations $\langle N_{\text{ch}}^{pp} \rangle_{1,2}$ and $\langle N_{\text{ch}}^{AA} \rangle_{1,2}$ in $p + p / A + A$ collisions. In general, Figs. 1a, b demonstrate that the curves for $z_{\pi}^{(n)}$ show the close behavior for various $\langle N_{\text{ch}}^{pp} \rangle$, especially at larger X . The clear increase of $z_{\pi}^{(n)}$ is observed with growth of energy in the case of the approximation $\langle N_{\text{ch}}^{AA} \rangle_1$ (Fig. 1a) whereas there is almost no dependence $z_{\pi}^{(n)}$ vs energy for $\langle N_{\text{ch}}^{AA} \rangle_2$ especially at $X = 5$ in the domain with the presence of BEC effect (Figs. 1b). Values of $z_{\pi}^{(n)}$ are noticeably larger for calculations at $X = 2$ with equation $\langle N_{\text{ch}}^{pp} \rangle_2$ than that for the approximation $\langle N_{\text{ch}}^{pp} \rangle_1$ in any considered cases of parameterization for $\langle N_{\text{ch}}^{AA} \rangle$ vs energy. This discrepancy is some clearer for the function $\langle N_{\text{ch}}^{AA} \rangle_2$ in the domain $E_N \gtrsim 10^{19}$ eV (Fig. 1b). As expected, the features of the behavior of $\Delta z_{\pi}^{(n)}$ in dependence on energy parameters (Figs. 1c, d) are the same as well as the above observations for $z_{\pi}^{(n)}$ due to relation (3). Thus within the special case of the gPLM the both parameters $z_{\pi}^{(n)}$ and $\Delta z_{\pi}^{(n)}$ show the increase of pion yield for the case of presence of BEC and magnitude of this increase does not contradict, at least, at qualitative level to the muon excess observed in the collisions of ultra-high energy cosmic ray (UHECR) particles [33].

III. SUMMARY

The research programs of the large experiments at RHIC and the LHC open a multimessenger era for the physics of strong interaction.

In $p + p$ collisions at the LHC jet production is studied up to TeV-region in jet p_T and virtuality scale Q . Measurements of jet cross sections and strong coupling α_S are well agree with QCD calculations. Direct observation of dead cone effect supports the feature of the evolution of parton shower for heavy quarks predicted by QCD. The difference observed between ridge yield in low-multiplicity $p + p$ events at the LHC and in e^+e^- annihilation at LEP energies indicates on the additional processes for particle production in $p + p$ interactions. Enormous efforts on theory and experiment for nuclear collisions during last decades resulted in, with strong help of the study of collective effects, to the ‘‘Standard model’’ of (heavy) ion interactions at high energies. The cross sections are measured for top pair production in $p + \text{Pb}$ and $\text{Pb} + \text{Pb}$ collisions in multi-TeV energy domain. A global Bayesian analysis of jet and jet substructure data from RHIC and the LHC allows the extraction of the sQGP transport coefficient \hat{q}/T^3 which smooth decrease from on about 6.5 to 4.0 at increase of T from 0.15 to 0.50 GeV.

A key development during recent time was the democratization of initial state models that can reproduce experimental data for azimuthal anisotropy coefficients. The study of elliptic flow allows the new method which images the nuclear global shape by colliding them at ultra relativistic speeds and analysing the collective response of outgoing debris. The highest ever values of anisotropic and radial flow in heavy-ion collisions are achieved at the LHC with radial-flow velocities up to about $0.7c$ and light hadron v_2 measurements, which determine the magnitude of elliptic flow, are 30% higher than at the top RHIC energy. Measurements in collisions of small systems have found signatures of sQGP similar to those observed in large systems. Extensive and various studies allow the indication on the CME and CMW signals in Au + Au collisions with the upper limit for the first case $\sim 10\%$ from isobar Ru + Ru and Zr + Zr collisions. Direct studies for the existence of CME and CMW in heavy-ion collisions revealed that background effects are dominating at the LHC with the upper limit for the first case $\sim 20\%$ in Pb + Pb collisions at $\sqrt{s_{NN}} = 5.02$ TeV.

At present femtoscopic correlations are actively studied for very wide set of particle species including charmed mesons and light nucleus. Taking into account the femtoscopic results for $p - \Xi$ lead to mass–radius dependence for NS which agree with astrophysical data. Possibly, the BEC may affect on soft pion production in, at least, heavy nucleus collisions in multi-TeV range of $\sqrt{s_{NN}}$. This phenomenon provides noticeable increase the mean values of particle density as well as total multiplicity of charged particles (pions). Aforementioned new feature of multiparticle processes can in the general case contribute to the muon yield recorded in collisions of UHECR particles with the

³ The superindex ‘‘(n)’’ means that the quantities are calculated with help of the average densities namely but not via the average total multiplicities.

atmosphere.

-
- [1] J. Campbell, J. Huston, F. Krauss, *The black book of quantum chromodynamics* (Oxford Univ. Press, 2018).
 - [2] M. Arslanodk et al., arXiv: 2303.17254 [nucl-ex], 2023. Also the referencies therein.
 - [3] S. Acharya S. et al. (ALICE Collab.), *Eur. Phys. J. C* **84**, 813 (2024). Also the referencies therein.
 - [4] G. Aad et al. (ATLAS Collab.), arXiv: 2404.06829 [hep-ex], 2024. Also the referencies therein.
 - [5] A. Hayrapetyan et al. (CMS Collab.), arXiv: 2405.10785 [hep-ex], 2024. Also the referencies therein.
 - [6] A. Hayrapetyan et al. (CMS Collab.), arXiv: 2405.18661 [hep-ex], 2024. Also the referencies therein.
 - [7] A. Hayrapetyan et al. (CMS Collab.), *Phys. Rev. Lett.* **133**, 071903 (2024).
 - [8] S. Navas et al. (Particle Data Group), *Phys. Rev. D* **110**, 030001 (2024).
 - [9] V. A. Okorokov, *J. Phys. Conf. Ser.* **1690**, 012006 (2020).
 - [10] V. A. Okorokov, *Phys. At. Nucl.* **86**, 742 (2022).
 - [11] T. Bose et al., arXiv: 2209.13128 [hep-ph], 2022.
 - [12] R. M. Harris, E. G. Guler, Y. Guler, arXiv: 2202.03389 [hep-ex], 2022.
 - [13] V. A. Okorokov, *Proc. XXX International workshop on high energy physics* (World Scientific, 2015), p. 216.
 - [14] G. Aad et al. (ATLAS Collab.), *JHEP* **2024**, 101 (2024).
 - [15] A. M. Sirunyan et al. (CMS Collab.), *Phys. Rev. Lett.* **119**, 242001 (2017).
 - [16] A. M. Sirunyan et al. (CMS Collab.), *Phys. Rev. Lett.* **125**, 222001 (2020).
 - [17] G. Aad et al. (ATLAS Collab.), arXiv: 2411.10186 [hep-ex], 2024.
 - [18] V. A. Okorokov, *Int. J. Mod. Phys. E* **22**, 1350041 (2013).
 - [19] V. A. Okorokov, *Yad. Fiz.* **80**, 652 (2017) [*Phys. At. Nucl.* **80**, 1133 (2017)].
 - [20] M. I. Abdulhamid et al. (STAR Collab.), *Nature* **635**, 67 (2024).
 - [21] M. I. Abdulhamid et al. (STAR Collab.), *Phys. Rev. Res.* **6**, L032005 (2024).
 - [22] M. I. Abdulhamid et al. (STAR Collab.), *Phys. Rev. C* **110**, 014905 (2024).
 - [23] M. S. Abdallah et al. (STAR Collab.), *Phys. Rev. Lett.* **128**, 092301 (2022).
 - [24] J.-H. Chen et al., *Nucl. Sci. Tech.* **35**, 214 (2024).
 - [25] L. Fabietti, V. Mantovani Sarti, O. Vázquez, *Annu. Rev. Nucl. Part. Sci.* **77**, 377 (2021).
 - [26] J. Adam et al. (STAR Collab.), *Phys. Lett. B* **790**, 490 (2019).
 - [27] S. Pratt, *Phys. Lett. B* **301**, 159 (1993).
 - [28] T. Csörgö, J. Zimányi, *Phys. Rev. Lett.* **80**, 916 (1998).
 - [29] J. Zimányi, T. Csörgö, *Acta Phys. Hun. New Serie Heavy Ion Phys.* **9**, 241 (1999).
 - [30] J. Adam et al. (ALICE Collab.), *Phys. Rev. C* **93**, 054908 (2016).
 - [31] V. A. Okorokov, *Adv. High Energy Phys.* **2016**, 5972709 (2016).
 - [32] V. A. Okorokov, *Phys. At. Nucl.* **82**, 838 (2019).
 - [33] V. A. Okorokov, *Phys. At. Nucl.* **87**, 172 (2024).

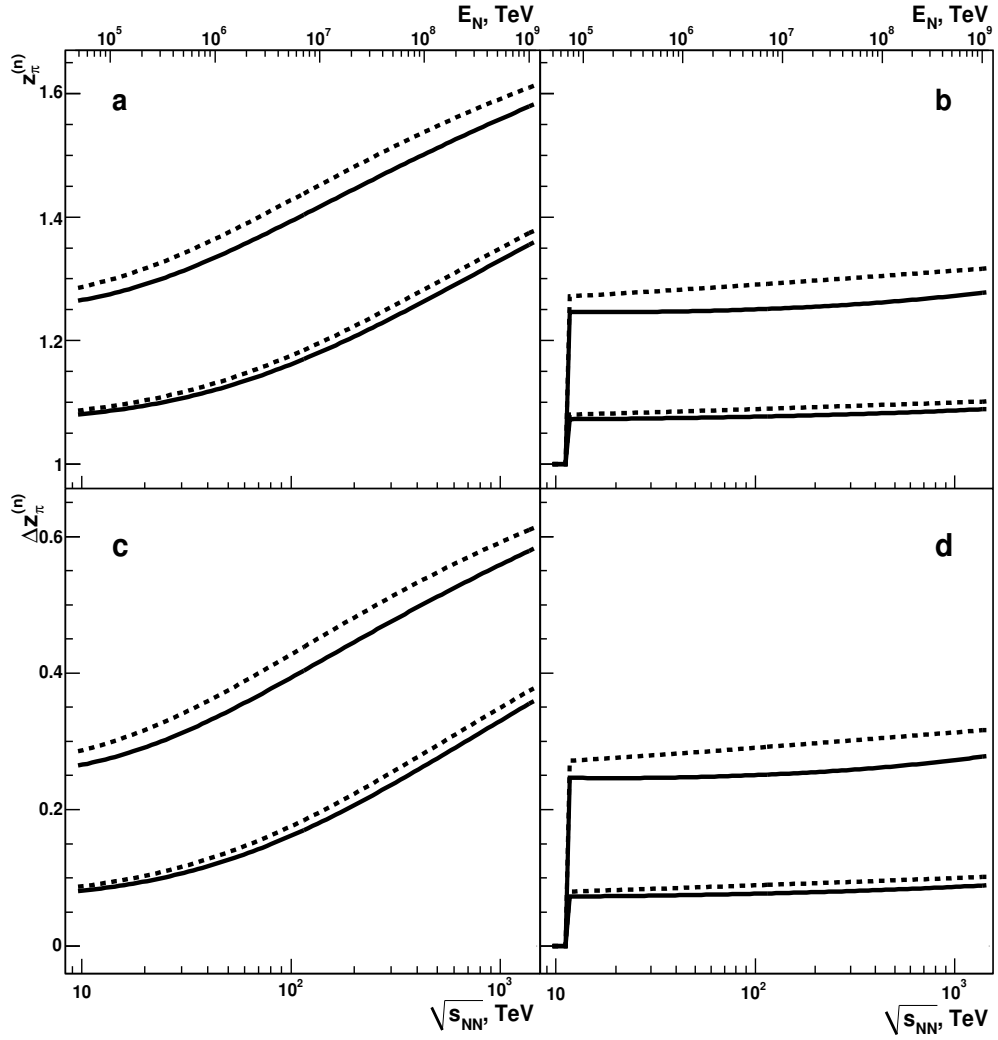


FIG. 1: Parameters $z_{\pi}^{(n)}$ (a, b) and $\Delta z_{\pi}^{(n)}$ (c, d) in dependence on energy. In the case of a symmetric ($A + A$) ion collisions the approximation $\langle N_{ch}^{AA} \rangle_1$ is used for the panels (a, c) while $\langle N_{ch}^{AA} \rangle_2$ is used for the panels (b, d). In each panel solid lines correspond to the $\langle N_{ch}^{pp} \rangle_1$, dashed lines are for $\langle N_{ch}^{pp} \rangle_2$. Effect of BEC is taken into account in accordance with the relation for the mean value $n(X)$ shown in the main text for energy region with $\langle n_{ch} \rangle > n_{ch,c}$ in certain type of collisions if any. The upper collection of curves are for $X = 2$, lower curves are for $X = 5$ [33].